Tanzania Journal of Science 47(3): 953-968, 2021
ISSN 0856-1761, e-ISSN 2507-7961

An Age-Structured Model for Transmission Dynamics of Malaria with Infected Immigrants and Asymptomatic Carriers

Asha S Kalula[1,2*], Eunice Mureithi [1], Theresia Marijani[1] and Isambi Mbalawata[3]
[1] Department of Mathematics, University of Dar es Salaam, P. O. Box 35062, Tanzania.
[2]Department of Mathematics, Physics and Information, Mkwawa University College of Education, P. O. Box 2513, Tanzania.
[3]African Institute for Mathematical Sciences (AIMS), Cellule Kamatamu, Rue KG590 ST No 1 Kigali, Rwanda.
**Corresponding author, email: kalulaasha@gmail.com*
Co-authors' emails: ewambui02@gmail.com, tmarijani@gmail.com, imbalawata@nexteinstein.org
Received 22 Jan 2021, Revised 30 Jun 2021, Accepted 20 Jul 2021, Published Aug 2021
DOI: https://dx.doi.org/10.4314/tjs.v47i3.7

Abstract

An age-structured (children and adults) model for the transmission dynamics of malaria with asymptomatic carriers and infected immigrants has been analyzed. We first analyze a model without infected immigrants. It shows that the disease-free equilibrium exists and is stable when $R_0 < 1$ and unstable for $R_0 > 1$. Also, we compute the sensitivity indices of the basic reproduction number. The basic reproduction number is most sensitive to the mosquito biting rate. Besides, the sensitivity of the basic reproduction number shows that the children's class parameters are more sensitive than those of adults. In the presence of infected immigrants, the model does not admit a disease-free equilibrium. The sensitivity of endemic equilibrium shows that the asymptomatic carrier parameters are more critical than that of infected immigrants. Also, the inflow of infectious immigrants is sensitive than that of infected immigrants. The results obtained indicate that strategies that target asymptomatic carriers and infected immigrants can help control malaria.

Keywords: Age-structure, malaria, immigrants, asymptomatic carrier, nonlinear ODE model.

Introduction

Malaria is a life-threatening vector-borne disease caused by a *Plasmodium* parasite and transmitted to humans by infected female *Anopheles* mosquito. Despite the efforts to prevent, control, and eradicate the disease, malaria is a public health problem globally and mainly in the tropics and subtropics regions. In 2019, malaria was estimated to be 229 million cases and 409000 deaths worldwide (WHO 2019). The disease is more severe to children under five years old, with two-thirds of the reported deaths being children (WHO 2019).

Several factors contribute to malaria transmission. These include infected immigrants, asymptomatic carriers and age. Malaria burden depends on the age-structure of the human population as children under five years old bear more burden than adults (WHO 2019). Children under five years are more vulnerable to malaria than adults since they have not developed immunity to infections (Schumacher and Spinelli 2012). Hence, age-structure is an important factor for the transmission of malaria in a population. Immigration contributes to the spread, reemergence and introduction of the parasite

into the community (Martens and Hall 2000). Asymptomatic carriers are individuals who have lower parasite density and do not show symptoms (Babiker et al. 2013). Asymptomatic infections occur as a result of repeated exposure to disease (Cai et al. 2017). The asymptomatic carrier serves as a reservoir of parasites for malaria transmission (Kern et al. 2011). Therefore, the inclusion of asymptomatic carriers in a model becomes important. Numerous mathematical models have been developed to quantify the impacts of immigrants, for instance, Tumwiine et al. (2010), Mukandavire et al. (2010) and Makinde and Okosun (2011), age by Addawe and Lope (2012a) and Forouzannia and Gumel (2014) and asymptomatic carriers in Águas et al. (2008) and Mandal et al. (2013). Apart from these studies on each factor, Filipe et al. (2007) and Mwanga et al. (2015) incorporated asymptomatic carriers and age. The studies with infected immigrants have shown not to have a disease-free equilibrium (Tumwiine et al. 2010, Mukandavire et al. 2010). With age structure, the study by Addawe and Lope (2012b) suggested that strategies to lower the number of bites on humans aged five years and below by using insecticide-treated nets (ITN's) and indoor residual spraying (IRS) would be considered to control the disease. Mwanga et al. (2015) analyzed an age-structured model with two classes and asymptomatic carriers on both classes in the presence of control strategies to obtain an optimal control strategy to control malaria. The control strategies used were long-lasting insecticide-treated nets, treatment of symptomatic and asymptomatic infectives and indoor residue spraying. Their results showed that the disease could be brought to stable disease equilibrium when all four controls are used. However, none of these studies considered age, infected immigrants and asymptomatic carriers. The model formulated in this study is an extension of the model by Forouzannia and Gumel (2014), which included asymptomatic carriers and infected immigrants. Unlike in Mwanga et al. (2015), the model considered here comprises of individuals who can contract the disease (susceptible), individuals who have been infected but not infectious (exposed), infectious individuals who are capable of transmitting the disease (infectious) and the recovered are individuals with temporary immunity- (SEIR). Since malaria burden is more to children below five years (WHO 2019) and symptomatic is higher for a lower age (Mandal et al. 2013), we assume that individuals below five years are only symptomatic. Therefore, asymptomatic carriers in this study are only in the adult class. However, it has been shown that children living in the area with moderate and high malaria transmission may become asymptomatic from three years (Wamae et al. 2019). The model also incorporates infected immigrants.

This study develops an age-structured mathematical model incorporating infected immigrants and asymptomatic carriers to understand their combined effects on malaria transmission dynamics.

Materials and Methods

The current study used a flow diagram (Figure 1) to describe the movements of humans and mosquitoes from one compartment to another depending on their disease status. The flow diagram was then used to formulate an age-structured mathematical model for malaria transmission that incorporates infected immigrants and asymptomatic carriers.

Model formulation

The model with human and mosquito compartments is formulated as follows: The human population N_h is divided into two classes, children N_c and adults class N_a ; that is $N_h = N_c + N_a$. The children class is a subgroup of the host population whose members are less than five years old. These members are vulnerable to the disease. The adult class is the group of individuals aged five years and above. The idea of grouping the human population into children and adults is consistent with other studies by Forouzannia and Gumel (2014), Addawe and Pajimola

(2016) and Okuneye and Gumel (2017). We group the human population into children and adults because children are more prone to malaria than those aged five years and above. Each group is further subdivided into four classes; the susceptible S, exposed E, infectious I and recovered class R. The infectious class for adults is then divided into asymptomatic A_a and symptomatic I_a. The asymptomatic class represents individuals who are infectious but do not show symptoms. These individuals are not affected by the disease but can transmit it to mosquitoes.

On the other hand, the symptomatic class (I_a) represents infectious individuals who show symptoms, can infect and are themselves affected by the disease. The classes are categorized with subscript c for individuals aged below five years and with subscript a for individuals with five years and above. Hence, the total human population $N_h = S_c + E_c + I_c + R_c + S_a + E_a + I_a + A_a + R_a$. The rate of infections of a susceptible individual is dependent on the mosquito's biting rate b and the proportion of bites by infectious mosquitoes on susceptible humans (β_c, β_a) that produce infections for children and adults, respectively. Upon infections, children and adults move to the exposed class E_c and E_a, respectively; at this stage, individuals cannot transmit the disease to susceptible mosquitoes since they do not have gametocytes. Exposed children and adults progress at a rate σ_c and σ_a respectively to infectious class in which they can infect susceptible mosquitoes because they have gametocytes in their bloodstream. For the exposed compartment in the adult group, a proportion θ $(0 < \theta < 1)$ progresses to symptomatic class and the remaining $(1 - \theta)$ joins the asymptomatic class. A proportion ϕ of symptomatic adult recovers at a rate γ_s and the remaining $(1 - \phi)$ joins the asymptomatic class at a rate α upon developing partial immunity due to continuous exposure to malaria. Asymptomatic individuals may recover naturally with temporary immunity at a rate γ_a and children may recover through treatment or naturally with temporary immunity at a rate γ_c. The recovered individuals with temporary immunity lose immunity and become susceptible at a rate η_c for children and η_a for adults. Individuals in every compartment suffer natural death at a rate μ. Individuals in the infectious class suffer disease-induced death at a rate δ except for the asymptomatic class who are not affected by the disease. The disease-induced death rate for children is δ_c and for adults is δ_a. The per capita birth rate for human is Λ_c and the immigration rate is π. We assume that immigrants are only adults for simplicity, whereby a fraction ρ_1 of immigrants are exposed, a fraction ρ_2 are asymptomatic, and the remaining fraction $(1 - \rho_1 - \rho_2)$ are susceptible. We also assume that children mature and join the corresponding adult class at a rate ζ.

The adult mosquito population is divided into three compartments: susceptible S_m, exposed E_m and infectious I_m. Thus, the total mosquito population $N_m = S_m + E_m + I_m$. The per capita recruitment rate for mosquitoes is Λ_m. The infection rate of a susceptible mosquito depends on the mosquito's biting rate b and the proportion of bites by susceptible mosquitoes on infected humans, resulting in infection β_m. We assume that A_a are less infectious than I_c and I_a by a factor r $(i.e., 0 < r < 1)$. During blood meals, susceptible mosquitoes take up gametocytes from infectious humans and move to the exposed class. At this stage, mosquitoes do not have sporozoites in their salivary gland and therefore are not contagious. When gametocytes developed into sporozoites, mosquitoes are considered infectious and move to infectious class at a rate σ_m. We did not consider clearance of sporozoites in mosquitoes due to their life expectance (Chitnis et al. 2006, Addawe and Lope 2012a). In every class, mosquitoes die naturally at a rate μ_m and no disease-induced death since infected mosquitoes are not harmed by the infections.

Model assumptions

(i) The death related to the disease is different between children and adults (i.e., $\delta_c > \delta_a$).

(ii) Asymptomatic carriers have a low probability of infecting susceptible mosquitoes than symptomatic adults by a factor r, so that $0 < r < 1$. This is because symptomatic adults are more infectious than the asymptomatic carriers (Águas et al. 2008) and have low parasite density (Babiker et al. 2013).

(iii) There are no asymptomatic carriers in children class because malaria in children is always clinical due to a lack of immunity (Chiyaka et al. 2007, Schumacher and Spinelli 2012).

(iv) Asymptomatic carriers can recover naturally because of the low parasites in which immune response can effectively control and eliminate the parasites (Babiker et al. 2013).

(v) Symptomatic individuals can develop partial immunity and become asymptomatic.

(vi) No immigration for children (for simplicity) and in symptomatic (since they are sick (Chitnis et al. 2006)). The description of the model and assumptions lead to a compartmental diagram in Figure 1.

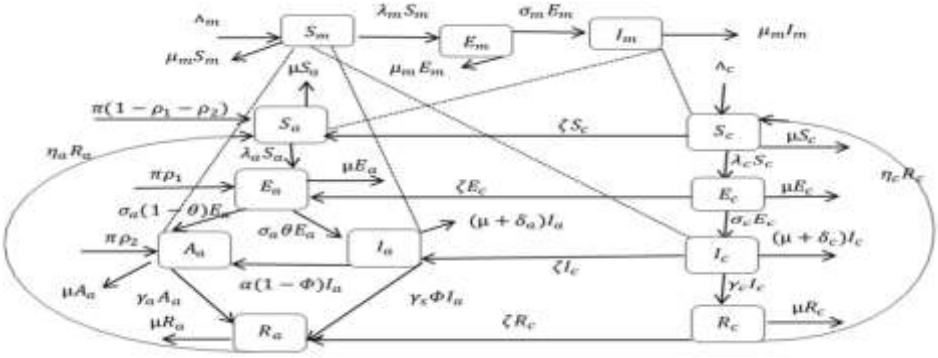

Figure 1: Flow diagram for the dynamics of malaria in the two age groups.

The bold arrows indicate individuals and mosquitoes' movements from one compartment to another, while the dash lines represent the interactions between humans and mosquitoes. Description of variables and parameters in the model are given in Table 1 and Table 2, respectively.

Table 1: Description of variables used in the model (1)

Variable	Description
S_c	Susceptible children aged below five years
E_c	Exposed children aged below five years
I_c	Infectious children aged below five years
R_c	Recovered children aged below five years
S_a	Susceptible adults aged five years and above
E_a	Exposed adults aged five years and above
I_a	Infectious adults aged five years and above with symptomatic malaria
A_a	Infectious adults aged five years and above with asymptomatic malaria
R_a	Recovered adults aged five years and above
S_m	Susceptible mosquitoes
E_m	Exposed mosquitoes
I_m	Infectious mosquitoes

Table 2: Description of parameters used in the model equation (1)

Parameter	Description
β_a	The probability of transmission from an infectious mosquito to a susceptible adult given that contact between the two occurs
β_c	The probability of transmission from an infectious mosquito to a susceptible child given that contact between the two occurs
β_m	The probability of transmission from an infectious human to a susceptible mosquito given that contact between the two occurs
λ_j, (j = c, a, m)	The infection rate for susceptible children, adult and mosquito
σ_j, (j = c, a, m)	Progression rate from the exposed to infectious class for children, adult and mosquito
π	Immigrants recruitment rate
γ_k (k = c, a, s)	The recovery rate of children, asymptomatic carriers and symptomatic individuals from malaria
r	Relative infectivity of I_a when compared to A_a
ζ	Maturation rate of children to adult
b	Average per capital biting rate of mosquitoes
η_c, η_a	Rate of loss of immunity for children and adult
δ_c, δ_a	Disease induced death rate for symptomatic malaria in children and adult
Λ_m, Λ_c	Mosquito recruitment rate and human per capita birth rate, respectively
ρ_1, ρ_2	The proportion of immigrants who are exposed and asymptomatic, respectively
θ	The proportion of exposed adults who show clinical symptoms
ϕ	The proportion of symptomatic adults who recover
μ, μ_m	The natural mortality rate for human beings and mosquitoes, respectively
α	The rate at which symptomatic adults become asymptomatic
m	Vector-human ratio $\frac{N_m}{N_h}$

Model equations

Based on the flow diagram in Figure 1 and the model parameters and variables provided in Table 1 and Table 2, respectively, the following system of ordinary differential equations (1) describes the dynamics of malaria in the two human sub-populations and the mosquito population.

Analysis of the model

In this section, we analyze the model (1) to get insights into malaria dynamics. Also, we use the model to assess the effects of age, immigrants, and asymptomatic carriers on malaria transmission.

$$\left.\begin{aligned}
\acute{S_c} &= \Lambda_c N_h + \eta_c R_c - (\mu + \lambda_c + \zeta) S_c, \\
\acute{E_c} &= \lambda_c S_c - (\mu + \sigma_c + \zeta) E_c, \\
\acute{I_c} &= \sigma_c E_c - (\mu + \delta_c + \zeta + \gamma_c) I_c, \\
\acute{R_c} &= \gamma_c I_c - (\mu + \zeta + \eta_c) R_c, \\
\acute{S_a} &= (1 - \rho_1 - \rho_2)\pi + \zeta S_c + \eta_a R_a - (\mu + \lambda_a) S_a, \\
\acute{E_a} &= \pi\rho_1 + \lambda_a S_a + \zeta E_c - [\mu + \sigma_a\theta + \sigma_a(1-\theta)] E_a, \\
\acute{I_a} &= \sigma_a\theta E_a + \zeta I_c - [\mu + \delta_a + \gamma_s\phi + \alpha(1-\phi)] I_a, \\
\acute{A_a} &= \pi\rho_2 + \sigma_a(1-\theta) E_a + \alpha(1-\phi) I_a - (\mu + \gamma_a) A_a, \\
\acute{R_a} &= \gamma_a A_a + \gamma_s\phi I_a + \zeta R_c - (\mu + \eta_a) R_a, \\
\acute{S_m} &= \Lambda_m N_m - (\mu_m + \lambda_m) S_m, \\
\acute{E_m} &= \lambda_m S_m - (\mu_m + \sigma_m) E_m, \\
\acute{I_m} &= \sigma_m E_m - \mu_m I_m, \\
\acute{N_h} &= \pi + (\Lambda_c - \mu) N_h - \delta_c I_c - \delta_a I_a, \\
\acute{N_m} &= (\Lambda_m - \mu_m) N_m,
\end{aligned}\right\} \quad (1)$$

where $\lambda_c = \frac{b\beta_c I_m}{N_h}$, $\lambda_a = \frac{b\beta_a I_m}{N_h}$ and $\lambda_m = \frac{b\beta_m [I_c + I_a + rA_a]}{N_h}$.

Existence of equilibrium

Before we investigate the existence of equilibrium points, we normalize the population in each class by dividing with their respective total populations (i.e., $e_c = \frac{E_c}{N_h}$, $e_a = \frac{E_a}{N_h}$, $e_m = \frac{E_m}{N_m}$ etc.) as in Chitnis et al. (2008) . Then differentiating with respect to t, we obtain $\frac{de_c}{dt} = \frac{1}{N_h}\left[\frac{dE_c}{dt} - e_c\frac{dN_h}{dt}\right]$, $\frac{de_a}{dt} = \frac{1}{N_h}\left[\frac{dE_a}{dt} - e_a\frac{dN_h}{dt}\right]$, $\frac{de_m}{dt} = \frac{1}{N_h}\left[\frac{dE_m}{dt} - e_m\frac{dN_h}{dt}\right]$. We repeat the process for the remaining variables. Solving for the derivatives of scaled variables and employing the technique by Tumwiine et al. (2010), we obtain

$$\left.\begin{aligned}
\acute{s_c} &= \Lambda_c + \eta_c r_c - (mb\beta_c i_m + \zeta + \mu) s_c \\
\acute{e_c} &= mb\beta_c i_m s_c - g_2 e_c, \\
\acute{\imath_c} &= \sigma_c e_c - g_3 i_c, \\
\acute{r_c} &= \gamma_c i_c - g_4 r_c, \\
\acute{s_a} &= (1 - \rho_1 - \rho_2)(\delta_a i_a + \delta_c i_c - \Lambda_c + \mu) + \eta_a r_a + \zeta s_c - (\mu + mb\beta_a i_m) s_a, \\
\acute{e_a} &= \rho_1(\delta_a i_a + \delta_c i_c - \Lambda_c + \mu) + \zeta e_c - (\mu + \sigma_a) e_a + mb\beta_a i_m s_a, \\
\acute{\imath_a} &= \sigma_a\theta e_a + \zeta i_c - g_1 i_a, \\
\acute{a_a} &= \rho_2(\delta_a i_a + \delta_c i_c - \Lambda_c + \mu) + \sigma_a(1-\theta) e_a + \alpha(1-\phi) i_a - (\mu + \gamma_a) a_a, \\
\acute{r_a} &= \gamma_a a_a + \gamma_s\phi i_a + \zeta r_c - (\mu + \eta_a) r_a, \\
\acute{s_m} &= \Lambda_m(1 - s_m) - b\beta_m(i_c + i_a + ra_a) s_m, \\
\acute{e_m} &= -\Lambda_m e_m - e_m\sigma_m + b\beta_m(i_c + i_a + ra_a) s_m, \\
\acute{\imath_m} &= \sigma_m e_m - i_m\Lambda_m
\end{aligned}\right\} \quad (2)$$

where, $g_1 = \delta_a - \alpha\phi + \alpha + \mu + \phi\gamma_s$, $g_2 = \sigma_c + \zeta + \mu$, $g_3 = \gamma_c + \delta_c + \zeta + \mu$, $g_4 = \eta_c + \zeta + \mu$, $m = \frac{N_m}{N_h}$, subject to the conditions $s_m + e_m + i_m = 1$, $s_c + e_c + i_c + r_c + s_a + e_a + i_a + a_a + r_a = 1$. All the feasible solutions of system (2) enter the region of biological interest defined by $\Omega = \{(s_c, e_c, i_c, r_c, s_a, e_a, i_a, a_a, r_a, s_m, e_m, i_m \in R_+^{12} : s_c, e_c, i_c, r_c, s_a, e_a, i_a, a_a, r_a, s_m, e_m, i_m \geq 0, s_c + e_c + i_c + r_c + s_a + e_a + i_a + a_a + r_a = 1, s_m + e_m + i_m = 1\}$.

We consider two scenarios; first, we analyze the model system (2) in the absence of infected immigrants (i.e., $\rho_1 = \rho_2 = 0$); and secondly, we analyze the model in the presence of infected immigrants (i.e., $\rho_1, \rho_2 > 0$).

Malaria transmission in the absence of infected immigrants

Substituting $\rho_1 = \rho_2 = 0$ in model equations (2), we obtain the model with only susceptible immigrants. Equating the derivatives in equations (2) equal to zero, we get the disease-free equilibrium (E_0) as

$$E_0 = (s_c^*, e_c^*, i_c^*, r_c^*, s_a^*, e_a^*, i_a^*, a_a^*, r_a^*, s_m^*, e_m^*, i_m^*) = \left(\frac{\Lambda_c}{\zeta+\mu}, 0,0,0, \frac{\zeta+\mu-\Lambda_c}{\zeta+\mu}, 0,0,0,0,1,0,0\right).$$

Basic reproduction number and local stability of the disease-free equilibrium *(E_0)*

The basic reproduction number R_0 represents the average number of secondary cases that one infected human (mosquito) can generate during the infection duration in a susceptible population. We determine the basic reproduction number R_0 using the next-generation matrix as described in Van den Driessche and Watmough (2002). The matrices for new infection terms (F) and the transfer terms (V) evaluated at E_0 are given by

$$F = \begin{pmatrix} 0 & 0 & 0 & 0 & 0 & 0 & \frac{mb\beta_c\Lambda_c}{\zeta+\mu} \\ 0 & 0 & 0 & 0 & 0 & 0 & 0 \\ 0 & 0 & 0 & 0 & 0 & 0 & \frac{mb\beta_a(\zeta+\mu-\Lambda_c)}{\zeta+\mu} \\ 0 & 0 & 0 & 0 & 0 & 0 & 0 \\ 0 & b\beta_m & 0 & b\beta_m & rb\beta_m & 0 & 0 \\ 0 & 0 & 0 & 0 & 0 & 0 & 0 \end{pmatrix},$$

$$V = \begin{pmatrix} g_2 & 0 & 0 & 0 & 0 & 0 & 0 \\ -\sigma_c & g_3 & 0 & 0 & 0 & 0 & 0 \\ \zeta & 0 & \mu+\sigma_a & 0 & 0 & 0 & 0 \\ 0 & -\zeta & -\theta\sigma_a & 0 & 0 & 0 & 0 \\ 0 & 0 & -(1-\theta)\sigma_m & -\alpha(1-\phi)\mu+\gamma_a & 0 & 0 & 0 \\ 0 & 0 & 0 & 0 & 0 & \Lambda_m+\sigma_a & 0 \\ 0 & 0 & 0 & 0 & 0 & -\sigma_a & \Lambda_m \end{pmatrix},$$

respectively. The reproduction number (R_0) represents the dominant eigenvalue of the generation matrix FV^{-1} which works to be:

$$R_0 = \sqrt{(R_c + R_a)R_m},$$

where

$$R_c = \frac{mb\beta_c\Lambda_c}{\zeta+\mu}\left\{\frac{\zeta r\sigma_m\left(\alpha(1-\phi)\sigma_c(\sigma_a+\mu) + g_3\sigma_a\left(\alpha\theta(1-\phi)+g_1(1-\theta)\right)\right)}{g_1g_2g_3(\sigma_a+\mu)(\gamma_a+\mu)} + \frac{(\sigma_c(\zeta+g_1)(\sigma_a+\mu)+\zeta g_3\theta\sigma_a)}{g_1g_2g_3(\sigma_a+\mu)}\right\},$$

$$R_a = \frac{mb\beta_a}{\zeta+\mu}\left\{\frac{r\sigma_a(-\Lambda_c+\zeta+\mu)\left(\alpha\theta(1-\phi)+g_1(1-\theta)\right)}{g_1(\gamma_a+\mu)(\sigma_a+\mu)} + \frac{\theta\sigma_a(-\Lambda_c+\zeta+\mu)}{g_1(\sigma_a+\mu)}\right\},$$

$$R_m = \frac{b\beta_m\sigma_m}{\Lambda_m(\Lambda_m+\sigma_m)}.$$

R_c is the number of secondary infections in children by one infectious mosquito, R_a is the number of secondary infections in adults by one introduced infectious mosquito and R_m is the number of secondary infections in mosquitoes by a newly introduced infectious

child or adult. Using Theorem 2 of Van den Driessche and Watmough (2002), the following result is established:

Theorem 1. The disease-free equilibrium point E_0, is locally asymptotically stable if $R_0 < 1$ and unstable otherwise.

Sensitivity analysis of R_0

The sensitivity analysis of R_0 is used to determine the relative importance of different factors contributing to disease transmission to best control it. Sensitivity indices of the basic reproduction number with respect to parameters are computed following the method by Chitnis et al. (2008). For instance, the normalized forward sensitivity of R_0 with respect to parameter β_m is defined and computed as $\Upsilon_{\beta_m}^{R_0} = \frac{\partial R_0}{\partial \beta_m} \times \frac{\beta_m}{R_0} = 0.5$, which does not depend on the values of parameters. The rest of the sensitivity indices are evaluated numerically using the parameter values in Table 3, and the results are presented in Figure 2.

Table 3: Parameter values used in the numerical simulations

Parameter	Range	Value	Units	Source
βa	0.24-0.64	0.27	$Days^{-1}$	Okuneye and Gumel (2017)
βm	0.02-0.64	0.64	$Days^{-1}$	Okuneye and Gumel (2017)
βc	0.24-0.64	0.27	$Days^{-1}$	Okuneye and Gumel (2017)
δa	0.00001-0.0004	0.0002	$Days^{-1}$	Okuneye and Gumel (2017)
δc	0.00001-0.0005	0.0005	$Days^{-1}$	Okuneye and Gumel (2017)
γa	0.0006-0.01	0.002	$Days^{-1}$	Okuneye et al. (2019)
γs	0.0014-0.011	0.01	$Days^{-1}$	Addawe and Lope (2012a)
γc	0.0014-0.03	0.0014	$Days^{-1}$	Addawe and Lope (2012b)
Λc	0.000027-0.00014	0.000097	$Days^{-1}$	Chitnis et al. (2008)
Λm	0.020-0.27	0.13	$Days^{-1}$	Chitnis et al. (2008)
α	0-1	0.05	$Days^{-1}$	Okuneye et.al (2019)
$\rho 1$	0-1	0.4		Assumed
$\rho 2$	0-1	0.4		Assumed
σa	0.06-0.203	0.07	$Days^{-1}$	Okuneye and Gumel (2017)
σc	0.06-0.203	0.203	$Days^{-1}$	Okuneye and Gumel (2017)
σm	0.029-0.33	0.1	$Days^{-1}$	Chitnis et al. (2008)
r	0-1	0.68		Assumed
μ	0.00003-0.00006	0.00004	$Days^{-1}$	Okuneye and Gumel (2017)
ζ	0.000144-0.000183	0.000183	$Days^{-1}$	Okuneye and Gumel (2017)
φ	0-1	0.4		Assumed
ηa	0.0014-0.011	0.0027	$Days^{-1}$	Addawe and Lope (2012a)
ηc	0.0014-0.011	0.0027	$Days^{-1}$	Addawe and Lope (2012b)
b	0.1-1.0	0.5	$Days^{-1}$	Okuneye and Gumel (2017)
θ	0-1	0.637		Assumed

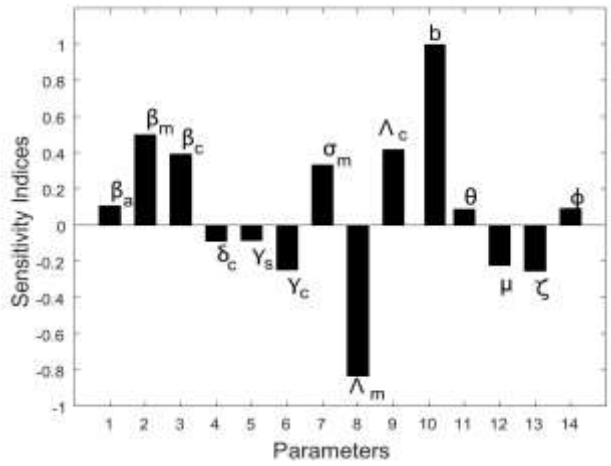

Figure 2: Sensitivity indices of R_0 with respect to the parameters.

The sign of sensitivity index in Figure 2 indicates whether R_0 is an increasing (or decreasing) function of the corresponding parameter. A positive index sign shows that R_0 is an increasing function of the corresponding parameter, whereas a negative sign shows that R_0 is a decreasing function of that parameter. The magnitudes of sensitivity indices indicate how sensitive R_0 is to the parameter. From Figure 2, the most sensitive parameter is the biting rate b followed by Λ_m, β_m , β_c , γ_c, Λ_c, σ_m and ζ. The sensitivity indices are in line with our expectation that decreasing the biting rate reduces the number of infected humans and mosquitoes and decreases disease transmission. Also decreasing β_m and β_c reduces the probability of mosquitoes and children being infected. Consequently, it reduces the number of infected mosquitoes and human beings, respectively, and reduces malaria transmission.

Existence of endemic equilibrium

The endemic equilibrium can be obtained by solving equation (2). However, the solution in a closed-form is not possible analytically. Using the parameter values in Table 3 when R_0 = 1.1370, we obtain numerical values for endemic equilibrium given by

$(s_c^*, e_c^*, i_c^*, r_c^*, s_a^*, e_a^*, i_a^*, a_a^*, r_a^*, s_m^*, e_m^*, i_m^*)$
$= (0.2395, 0.000169, 0.01531, 0.007049, 0.7077,$
$0.0009654, 0.002724, 0.002006, 0.02463,$
$0.9918, 0.005466, 0.002734).$

The stability of the endemic equilibrium is presented in Figure 4, whereby the proportion of the total number of infected humans (i.e., the sum of i_c, i_a and a_a) is plotted as a function of time with different initial conditions to show that the endemic equilibrium is stable when $R_0 > 1$.

A model with infected immigrants

To examine the combined effects of asymptomatic carriers and immigrants on an age-structured model, we now analyze the model system (2) with ρ_1 , $\rho_2 > 0$. The system has no disease-free equilibrium due to the presence of infected immigrants. The system's complexity has prevented us from finding an explicit solution for endemic equilibrium (EE). We, therefore, evaluate EE numerically using the parameter values in Table 3 to obtain (3)

$$(s_c^*, e_c^*, i_c^*, r_c^*, s_a^*, e_a^*, i_a^*, a_a^*, r_a^*, s_m^*, e_m^*, i_m^*) = (0.0071, 0.0010, 0.0944, 0.0435, 0.0317, 0.0141, 0.0188, 0.4473, 0.3421, 0.4933, 0.2864, 0.2203). \quad (3)$$

Sensitivity indices for the endemic equilibrium point

Sensitivity indices for the endemic equilibrium point are calculated using the method described by Chitnis et al. (2008). Since we cannot explicitly determine the endemic equilibrium, we use the system (2) and the endemic equilibrium values in equation (3). We replace the variables in the system (2) with proportions $x_1, x_2, x_3, x_4, x_5, x_6, x_7, x_8, x_9, x_{10}, x_{11}, x_{12}$ and the parameters $\beta_a, \beta_m, \beta_c, \delta_a, \delta_c, \gamma_a, \gamma_s, \gamma_c, \Lambda_c, \Lambda_m, \alpha, \rho_1, \rho_2, \sigma_c$ $\sigma_a, \sigma_m, r, \mu, \zeta, \phi, \eta_a, \eta_c, b, \theta, m$ by $p_1, p_2, p_3, p_4, p_5, p_6, p_7, p_8, p_9, p_{10}, p_{11}, p_{12}, p_{13}, p_{14}, p_{15}, p_{16}, p_{17}, p_{18}, p_{19}, p_{20}, p_{21}, p_{22}, p_{23}, p_{24}, p_{25}$. So the system (2) at equilibrium becomes

$$f_i(x_1, x_2, \ldots, x_{12}; p_1, p_2, \ldots, p_{25}) = 0, \quad (4)$$

where $i = 1, \ldots 12$. We need to compute $\frac{\partial x_j}{\partial p_k}$ with $j = 1, \ldots, 12$ and $k = 1, \ldots, 25$ for parameter values in Table 3 and the endemic equilibrium (3). Differentiating the equilibrium equations (4) with respect to p_k we obtain

$$\frac{df_i}{dp_k} = \sum_{j=1}^{12} \frac{\partial f_i}{\partial x_j}\frac{\partial x_j}{\partial p_k} + \sum_{l=1}^{25} \frac{\partial f_i}{\partial p_l}\frac{\partial p_l}{\partial p_k} = 0, \quad (5)$$

for $i = 1, \ldots 12$ and $k = 1, \ldots 25$ in which $\frac{\partial p_l}{\partial p_k} = 0$ if $l \neq k$. Hence each equation in (5) reduces to

$$\sum_{j=1}^{12} \frac{\partial f_i}{\partial x_j}\frac{\partial x_j}{\partial p_k} = \frac{\partial f_i}{\partial p_k}. \quad (6)$$

The equation (6) can then be written as

$$AX_k = z_k \quad (7)$$

where A is a (12 x 12) Jacobin matrix of the system (3) with entries $\frac{\partial f_i}{\partial x_j^*}$,

$$X_k = \left[\frac{\partial x_1^*}{\partial p_k}, \frac{\partial x_2^*}{\partial p_k}, \frac{\partial x_3^*}{\partial p_k}, \frac{\partial x_4^*}{\partial p_k}, \frac{\partial x_5^*}{\partial p_k}, \frac{\partial x_6^*}{\partial p_k}, \frac{\partial x_7^*}{\partial p_k}, \frac{\partial x_8^*}{\partial p_k}, \frac{\partial x_9^*}{\partial p_k}, \frac{\partial x_{10}^*}{\partial p_k}, \frac{\partial x_{11}^*}{\partial p_k}, \frac{\partial x_{11}^*}{\partial p_k}\right]^T$$

and

$$z_k = \left[\frac{-\partial f_1}{\partial p_k}, \frac{-\partial f_2}{\partial p_k}, \frac{-\partial f_3}{\partial p_k}, \frac{-\partial f_4}{\partial p_k}, \frac{-\partial f_5}{\partial p_k}, \frac{-\partial f_6}{\partial p_k}, \frac{-\partial f_7}{\partial p_k}, \frac{-\partial f_8}{\partial p_k}, \frac{-\partial f_9}{\partial p_k}, \frac{-\partial f_{10}}{\partial p_k}, \frac{-\partial f_{11}}{\partial p_k}, \frac{-\partial f_{12}}{\partial p_k}\right]^T$$

with $i = 1, \ldots 12$and $k = 1, \ldots 25$. Solving the system (7), we obtain the required X_k where A is evaluated at endemic equilibrium (3) and z_k with the parameter values in Table 3. Finally multiplying X_k by $\frac{p_k}{x_j}$, we obtain sensitivity indices of endemic equilibrium with respect to parameters. Table 4 represents sensitivity indices for i_c, i_a and a_a.

Interpretation of sensitivity indices of the endemic equilibrium

The five most sensitive parameters for endemic equilibrium, i_c are $\Lambda_c, \delta_c, \zeta, \mu$ and γ_c, for $i_a$are $\theta, \alpha, \phi, \gamma_a$and $\eta_a$and for a_a are $\gamma_a, \eta_a, \Lambda_c, \delta_c$ and ϕ. The direction of the sensitivity indices of the endemic equilibrium with respect to most of the parameters is consistent with the intuitive expectation except for the Λ_m which we expect that as mosquitoes are increased, the number of infected humans will also increase. An explanation for counterintuitive expectation is that an increase in the number of mosquitoes would affect the total number of mosquito bites on humans, hence reducing the number of infected humans. The least sensitive parameter for endemic equilibrium is the proportion of immigrants who are infective but not infectious ρ_1.

Table 4: Sensitivity indices of the endemic equilibrium for infectious individuals

	i_c	i_a	a_a
βa	0.00000	0.00218	0.002103
βm	0.00067	0.00116	0.00113
βc	0.00138	0.00022	0.00023
δa	-0.000003019	-0.01010	-0.00583
δc	-0.511768	0.07611	0.08872
γa	-0.000205218	0.51204	-0.46999
γs	-0.00001735445	-0.08104	-0.03207
γc	-0.16361	-0.03018	-0.03067
Λc	1.02437	-0.15308	-0.17838
Λm	-0.00144452	-0.00252	-0.002445
α	-0.00000087021	-0.93039	0.05554
$\rho 1$	0.00000004821950	0.000100	0.000097
$\rho 2$	0.000000397061	-0.04487	0.00361
σa	0.0013266246	0.000215	0.00022
σc	0.00002571585	0.053490	0.05164
σm	0.000778021	0.00136	0.001328
r	0.000487464	0.00085	0.00083
μ	-0.23008	0.07926	0.06547
ζ	-0.26650	0.06020	0.04517
φ	-0.00001677426	0.53922	-0.06910
ηa	0.0002044560	0.42527	0.41054
ηc	0.14237	0.02633	0.02675
b	0.0020429	0.00356	0.003458
θ	0.000000970378	1.03747	-0.06193
m	0.001376502	0.00240	0.00233

Results and Discussion

Numerical simulations of the model equations (2) were carried out to verify the analytical results obtained on the stability of equilibrium points. The models are simulated using fourth-order Runge Kutta in Matlab. All figures are generated using parameter values given in Table 3 obtained from different kinds of literature. Considering the model without infected immigrants, when $R_0 < 1$, for $R_0 = 0.9972$, the proportion of total infected individuals converges to the disease-free equilibrium as shown in Figure 3.

Figure 4 shows the dynamics of the model for $R_0 = 1.1370$, where the proportion of the total number of infected individuals tends to the endemic equilibrium point, which indicates the persistence of disease in the community when $R_0 > 1$.

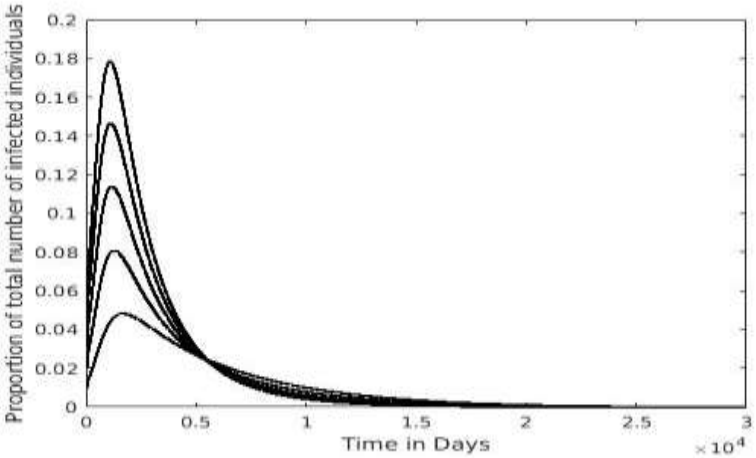

Figure 3: Simulation of the model without infected immigrants for $R_0 = 0.9972$ using various initial conditions.

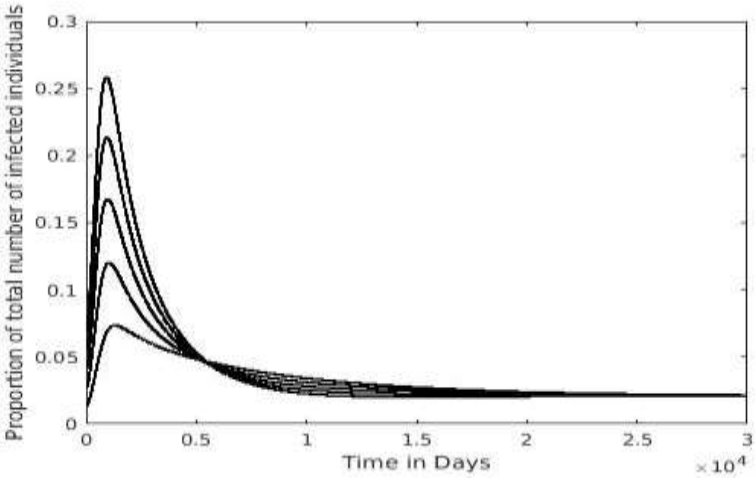

Figure 4: Simulation of the model without infected immigrants for $R_0 = 1.1370$, showing the proportion of the total number of infected individuals as a function of time using various initial conditions.

With the model that incorporated infected immigrants, Figure 5 represents the dynamics of infectious children, adults, and mosquitoes. The results show that all populations persist throughout the disease's duration, which suggests the existence of an endemic equilibrium point. Thus, no disease-free equilibrium exists, as shown analytically.

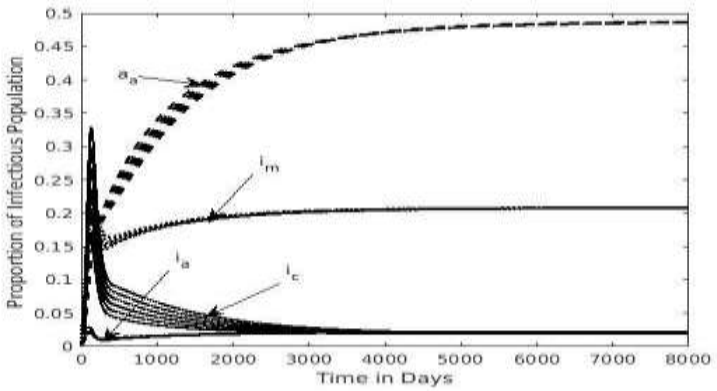

Figure 5: Long term dynamics of infectious children, adults and mosquito population, with parameter values defined in Table 3 and five different initial conditions were used.

Effects of infected immigrants and asymptomatic carriers

Here we assess the impacts of infected immigrants and asymptomatic carriers on an age-structured model (2) numerically. We compare the dynamics of the model with and without infected immigrants and asymptomatic carriers. The age-structured model without infected immigrants and asymptomatic carriers is determined by setting $r = \rho_1 = \rho_2 = a_a = 0, \phi = \theta = 1$ in the system (2). The results are presented in Figure 6 (a) in four cases. Case 1 is the prevalence of the age-structured model in the absence of infected immigrants and asymptomatic carriers. Case 2 is the prevalence of an age-structured model with infective immigrants (i.e. $\rho_1 > 0$ but $\rho_2 = 0$). Case 3 is the prevalence of an age-structured model with asymptomatic carriers. Case 4 is the prevalence of an age-structured model (2) with both infected immigrants and asymptomatic carriers. Figure 6 (a) shows that the pick of prevalence increases as we incorporate more factors as expected. This is because the population with no inflow of infected individuals and the asymptomatic carrier would have fewer malaria cases than those with infected immigrants and asymptomatic carriers. The observation implies that including more factors contributing to the malaria dynamics improves our understanding and helps determine the control strategies to contain the disease. Figure 6 (b) represents the prevalence of malaria with four cases which shows how prevalence varies with the model's changes. Case 1 is when model (2) is reduced to have the adult population only without children, immigrants and asymptomatic carriers. The case is obtained by setting $s_c = e_c = i_c = r_c = 0, \Lambda_c = \beta_c = \delta_c = \eta_c = \sigma_c = \gamma_c = \rho_1 = \rho_2 = r = a_a = 0$ and $\phi = \theta = 1$. In case 2, we have a model in case 1 incorporating infective immigrants ($\rho_1 = 0.4$). Case 3 is the model with asymptomatic carrier $r =$ 0.68, $\phi = 0.4, \theta = 0.637$, $\alpha = 0.05, \gamma_a = 0.002$, whereas case 4 includes both infected immigrants and children classes $\beta_c = 0.27$, $\delta_c = 0.0005$, $\eta_c = 0.0027$, $\delta_c = 0.203, \Lambda_c = 0.000097, \gamma_c = 0.0014$.

Furthermore, in the two figures, Figure 6 (a & b) case 1, represents the prevalence of malaria in an age-structured and adult-only model, respectively. Case 2 includes infective immigrants in both figures, and Case 3 incorporates asymptomatic carriers. This enables us to compare an age-structured and adult-only model with the inclusion of infected immigrants and asymptomatic carriers. We observe that an age-structured model has high peak than the model without age-structure in both cases.

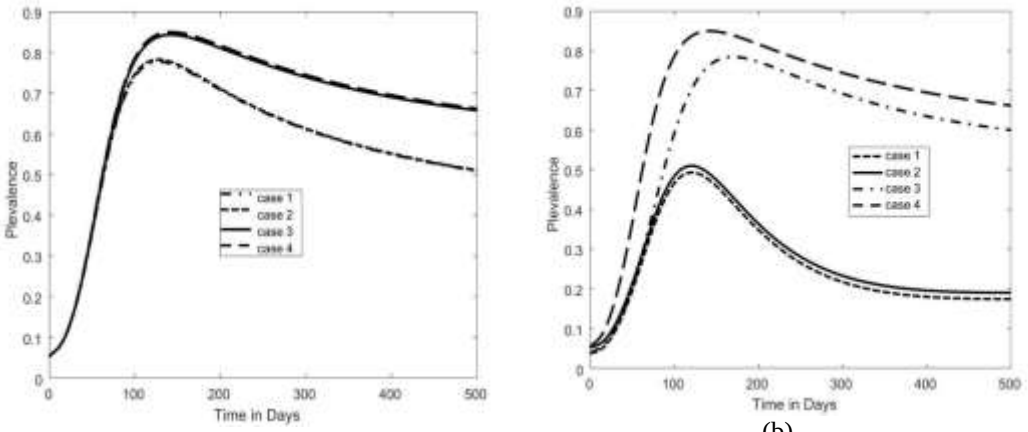

Figure 6: Malaria prevalence for different cases. In (a): Case 1 is an age-structure only, Case 2 is an age-structure with infective immigrants, Case 3 shows an age-structure with asymptomatic carriers and Case 4, age-structure, immigrants (both infective and infectious) and asymptomatic carriers. In (b): Case 1 is for adults only (without asymptomatic carriers and immigrants), Case 2 has adults and infective immigrants, Case 3 includes adults, immigrants (both infective and infectious), and asymptomatic carriers, and Case 4 incorporates adults with asymptomatic carriers and immigrants, and children.

Conclusion

In this paper, a deterministic, age-structured model for malaria transmission incorporating infected immigrants and asymptomatic carriers was formulated. The model was used to assess their combined effects on malaria dynamics. The model was analyzed analytically without the inflow of infected immigrants. The basic reproduction number R_0 was calculated numerically and indicated that for the $R_0 < 1$, the disease-free equilibrium point is asymptotically stable. For $R_0 > 1$ the endemic equilibrium exists. Sensitivity analysis for R_0 reveals that the biting rate is the most important parameter; the same result was reported in Chitnis et al. (2008), which suggest that reducing it will reduce disease transmission. Also, we observe that malaria is more sensitive to children's parameters than the corresponding parameters in adults. These results are consistent with the observations by Addawe and Lope (2012a). Therefore, controlling the disease in children will have more impact than controlling the disease in adults. On the other hand, the model with the inflow of infected immigrants shows that there is no disease-free equilibrium, as in other studies that include the inflow of infected immigrants such as Tumwiine et al. (2010), Mukandavire et al. (2010) and Makinde and Okosun (2011). Sensitivity analysis of endemic equilibrium was carried out. The numerical results indicate that the asymptomatic carriers have more impacts than the infected immigrants on malaria dynamics. These results imply that the control strategies targeting asymptomatic carriers will significantly impact the reduction of prevalence compared to targeting infected immigrants. Furthermore, it has been observed that neglecting age, infected immigrants, and asymptomatic carriers underestimate malaria's transmission dynamics as both play significant roles in the transmission dynamics of malaria. Although the study helps us assess the combined effects of infected immigrants and asymptomatic carriers on an age-structured

malaria transmission dynamics model, the model can be extended to include immigrants and asymptomatic carriers in children and factors related to climate change, which have significantly contributed to the transmission of malaria.

Acknowledgements
This work was funded by a grant from the African Institute for Mathematical Sciences, with financial support from the Government of Canada, provided through Global Affairs Canada and the International Development Research Centre. The corresponding author also acknowledges with gratitude the Ministry of Education, Science and Technology-Tanzania for financial support.

Declaration: The authors declare that they have no conflicts of interest.

References

Addawe JM and Lope JEC 2012a Analysis of age-structured malaria transmission model. *Philippine Sci. Lett.* 5: 169–186.

Addawe JM and Lope JEC 2012b Sensitivity analysis of the age-structured malaria transmission Model. In AIP *Conference Proceedings* 1482: 47-53, American Institute of Physics.

Addawe J and Pajimola AK 2016 Dynamics of climate-based malaria transmission model with the age-structured human population. AIP *Conference Proceedings* 1782(1): 040002, AIP Publishing LLC.

Águas R, White LJ, Snow RW and Gomes MGM 2008 Prospects for malaria eradication in Sub Saharan Africa. *PloS One* 3(3): e1767, 1-6.

Babiker HA, Gadalla, AA and Ranford-Cartwright LC 2013 The role of asymptomatic *P. falciparum* parasitaemia in the evolution of antimalarial drug resistance in areas of seasonal transmission. *Drug Resistance Updates* 16(1-2): 1-9.

Cai L, Li X, Tuncer N, Martcheva M and Lashari AA 2017 Optimal control of a malaria model with asymptomatic class and superinfection. *Math. Biosci.* 288: 94-108.

Chitnis N, Cushing JM and Hyman JM 2006 Bifurcation analysis of a mathematical model for malaria transmission. *SIAM J. Appl. Math.* 67(1): 24-45.

Chitnis N, Hyman JM and Cushing JM 2008 Determining important parameters in the spread of malaria through the sensitivity analysis of a mathematical model. *Bull. Math. Biol.* 70(5):1272.

Chiyaka C, Garira W and Dube S 2007 Transmission model of endemic human malaria in a partially immune population. *Math. Comput. Model.* 46(5-6): 806-822.

Filipe JAN, Riley EM, Drakeley CJ, Sutherland CJ and Ghani AC 2007 Determination of the processes driving the acquisition of immunity to malaria using a mathematical transmission model. *PLoS Comput. Biol.* 3(12): e255, 1-12.

Forouzannia F and Gumel AB 2014 Mathematical analysis of an age-structured model for malaria transmission dynamics. *Math. Biosci.* 247: 80-94.

Kern SE, Tiono AB, Makanga M, Gbadoé AD, Premji Z, Gaye O, Sagara I, Ubben D, Cousin M, Oladiran F, Sander O and Ogutu B 2011 Community screening and treatment of asymptomatic carriers of Plasmodium falciparum with artemether lumefantrine to reduce malaria disease burden: a modelling and simulation analysis. *Malaria J.* 10(1): 210.

Makinde OD and Okosun KO 2011 Impact of chemo-therapy on optimal control of malaria with disease infected immigrants. *BioSystems* 104: 32-41.

Mandal S, Sinha S and Sarkar RR 2013 A Realistic host-vector transmission model for describing malaria prevalence pattern. *Bull. Math. Biol.* 75: 2499-2528.

Martens P and Hall L 2000 Malaria on the move: Human population movement and malaria transmission. *Emerging Infect. Dis.* 6(2): 103-109.

Mukandavire C, Musuka G, Magombedzea G and Mukandavire Z 2010 Malaria model

with immigration of infectives and seasonal forcing in transmission. *Int. J. Appl. Math. Comput.* 2(3): 1-16.

Mwanga GG, Haario H and Capasso V 2015 Optimal control problems of epidemic systems with parameter uncertainties: Application to a malaria two-age-classes transmission model with asymptomatic carriers. *Math. Biosci.* 261: 1-12.

Okuneye K and Gumel AB 2017 Analysis of a temperature-and rainfall-dependent model for malaria transmission dynamics. *Math. Biosci.* 287: 72-92.

Okuneye K, Eikenberry SE and Gumel AB 2019 Weather-driven malaria transmission model with gonotrophic and sporogonic cycles. *J. Biol. Dynamics* 13(sup1): 288-324.

Schumacher RF and Spinelli E 2012 Malaria in children. *Mediterr. J. Hematol Infect. Dis*. 4(1): e2012073.

Tumwiine J, Mugisha JYT and Lubobi LS 2010 A host-vector model for malaria with infectives immigrants. *J. Math. Anal. Appl.* 361(1):139-149.

Van den Driessche P and Watmough J 2002 Reproduction numbers and sub-threshold endemic equilibria for compartmental models of disease transmission. *Math. Biosci.* 180: 29-48.

Wamae K, Wambua J, Nyangweso G, Mwambingu G, Osier F, Ndung'u F, Bejon P and Ochola-Oyier LI 2019 Transmission and age impact the risk of developing febrile malaria in children with asymptomatic *Plasmodium falciparum* parasitemia. *J. Infect. Dis.* 219(6): 936-944.

WHO (World Health Organization) 2019. World malaria report of 2019.